# A Low-Profile, Low-Cost Antenna System with Improved Gain for DSRC Vehicle-to-Vehicle Communications

**Michael Westrick,[1] Mohammad Almalkawi,[1] Vijay Devabhaktuni,[1] Charles Bunting[2]**

[1] Department of Electrical Engineering and Computer Science, MS 308, The University of Toledo, 2801 W. Bancroft Street, Toledo, OH 43606
[2] Department of Electrical and Computer Engineering, Oklahoma State University, 202 Engineering South, Stillwater, OK 74078

*Received 7 December 2011; accepted 15 March 2012*

**ABSTRACT: A novel wire antenna for future dedicated short range communications vehicle-to-vehicle communications is introduced. The proposed antenna carries low-profile and low-cost features, and possesses an improved gain performance. This article also includes a specific feed network design for the proposed antenna to meet the mechanical and manufacturing requirements. Two different numerical techniques using CST Microwave Studio and HFSS have been applied for evaluating the performance of the proposed antenna. The whole system including the feed network and the antenna elements is integrated, and its performance is also assessed.** © 2012 Wiley Periodicals, Inc. Int J RF and Microwave CAE 23:111–117, 2013.

**Keywords:** dedicated short range communications; feed network; gain; low-cost; low-profile; vehicle antenna

## I. INTRODUCTION

Modern automobile antennas are typically designed for frequencies suitable for FM/AM radio, global system for mobile communications, and global positioning system (GPS) communications, among others. Normally, the highest frequency antenna in a modern vehicle transmits at 2.4 GHz for Bluetooth [1]. In July 2010, IEEE amended the 802.11 standard with 802.11p, which regulated the frequency range of 5.85–5.925 GHz for wireless access in vehicle environments and dedicated short range communications (DSRC) [2]. Specifically, these include vehicle-to-vehicle and vehicle-to-infrastructure communications among other potential applications [3].

Because of various vehicle designs, manufacturing requirements, and electromagnetic compatibility constraints, which arise from the increased installations of several on-board electronics such as mobile telephones, Bluetooth transmitters, and radio frequency identification tags, automobile antennas require installation flexibility at different positions of the vehicle. For example, an antenna may be installed on the top of the car roof [4, 5], along the pillar [6, 7], on the surface of the windows [8], and even on the dashboard [9]. However, it is desirable for vehicle antennas to have the lowest possible profile to avoid cosmetically altering the vehicle's exterior appearance and to facilitate quick and easy installation [9]. Moreover, current automobile antennas operate at relatively low frequencies. At these frequencies, the physical length of a quarter-wavelength antenna is quite large. Thus, different technologies have been used to reduce antenna size. High-permittivity dielectric materials are used for automobile GPS antennas [10].

PIFA antennas [11] have been utilized for mobile handset technology. At FM/AM radio frequency bands, low-profile blade or shark fin antennas have been invented [12, 13]. Traditional wire antennas at these frequencies have lost their appeal due to the large physical dimensions necessary for the antennas to resonate at these low frequencies. However, in the DSRC frequency band, wire antennas would be able to regain the low-profile and low-cost advantages and provide the desired performance in their original size.

The objective of this article is to propose a novel configuration of a quarter-wavelength monopole antenna

Correspondence to: M. Almalkawi; e-mail: Mohammad.Almalkawi@rockets.utoledo.edu

DOI 10.1002/mmce.20657
Published online 11 May 2012 in Wiley Online Library (wileyonlinelibrary.com).

surrounded by parasitic elements for generating an omnidirectional radiation pattern. It will be shown that the proposed antenna exhibits the desirable feature of compactness while achieving an enhanced omnidirectional gain performance.

In order for the antenna to operate properly in a practical vehicle environment, it will need a mechanical support to securely fasten it to the vehicle body. This support structure will be in close proximity to the antenna elements and may affect the system's performance. Therefore, the support system needs to be accounted for in the design process. In this work, a specific feed network board with a metal base is proposed to meet the mechanical requirements. The whole system is assembled, and its performance is analyzed.

The organization of this article is as follows. Section II describes the antenna configuration in an ideal setup (i.e., without the feed network and the metal base support structure). Section III demonstrates the feed network board details. Section IV assesses the performance of the fully integrated antenna while, conclusions are given in Section V.

## II. ANTENNA DESIGN

The specifications of the proposed antenna are listed in Table I. The target frequency is around 5.9 GHz. A quarter-wavelength monopole antenna at that frequency is around 10-mm long, which would meet the low profile requirements. As this application is a relatively narrow band service, the monopole antenna is a good candidate to provide the desired bandwidth. A wire monopole antenna offers vertical polarization when it is vertically oriented. The difficulties arise when we attempt to achieve a higher gain while maintaining an omnidirectional radiation pattern in the horizontal plane. One way to increase the gain in colinear antennas [14, 15] is to introduce a certain number of iterations of radiating elements. However, these elements and the half wavelength destructive phase shift eliminating mechanism [16] between the radiating elements will increase the antenna dimensions considerably, although it would keep the omnidirectional radiation pattern on the horizontal plane. Yagi-Uda antennas [17] can be tuned to obtain a high directive gain by including an amount of parasitic elements in line with the driven element along with a reflector on the opposite side of the driven element [18]. Thus, the gain is proportional to the number of the parasitic elements in the price of the antenna's physical size. More importantly, the gain of this type of antenna is highly directional in nature [19]. However, it has been demonstrated that the parasitic element can be utilized without a reflector element to increase the antenna gain. Some parasitic antennas were built on the top of a skirted conductive sleeve to steer the direction of vertical radiation [20]. Here, a monopole antenna is used as the driven element; however, in this case, the monopole was on a finite ground plane [21]. For automobile applications, the metal surface of a car roof is normally treated as an infinite ground plane for the vehicle antenna [4–6].

**TABLE I Antenna Specifications**

| Feature | Specification |
|---|---|
| Frequency band | 5.85–5.925 GHz |
| Polarization | Vertical |
| Radiation pattern | Omnidirectional in the horizontal plane |
| Gain | $\geq$ 5 dBi, as high as possible |

This article describes a monopole antenna with eight parasitic elements that maintains a low-profile and also exhibits an improved gain performance. Although monopole arrays have been proposed for use in roadside base stations [22], to the authors' knowledge they have not previously been investigated for use in vehicles at DSRC frequencies and with this new configuration.

Figure 1 illustrates the ideal antenna setup, consisting of eight cylindrical elements touching a perfectly conducting ground plane. The single driven element is located in the center and eight parasitic elements form a circle of radius ($S$) around the driven element. Each element lies on the circumference of the circle, and they are separated from each other by 45°. For better understanding of the antenna operation, an ideal setup of the antenna where an ideal ground plane at $\theta = 90°$ plane is introduced in this section. A fully integrated antenna with feed network and metallic base will be discussed in the following sections.

The proposed antenna can be considered as the combination of eight single pairs of the central feed element and a separate parasitic element. To keep this antenna low profile, only one iteration of parasitic elements was chosen. This is different from Yagi-Uda antennas, where up to 30 or more parasitic elements can be utilized. It was found that the spacing between the driven element and parasitic elements plays a vital role in obtaining the desired gain and the omnidirectional radiation pattern.

Full-wave EM simulations have been carried out using CST Microwave Studio and confirmed by ANSYS-HFSS for demonstrating the antenna operation and for obtaining the optimal antenna parameters as listed in Table II. Figure 2 shows the return loss ($S_{11}$) response of the antenna in Figure 1, exhibiting a 10-dB bandwidth of 200 MHz, which completely covers the DSRC frequency band from 5.85 to 5.925 GHz. The response is obtained using both CST and HFSS simulators, and it is clearly observed that the two solvers which are based on two different numerical techniques are in a good agreement.

Both the $E$-plane (i.e., elevation plane, where $\varphi = 0°$) and the $H$-plane (i.e., horizontal plane, where $\theta = 90°$) far-field radiation patterns of the antenna with its ideal setup were evaluated using CST. Figure 3 shows the change of the far-field radiation pattern in the $E$-plane corresponding to the different elements' spacings ($S$). For this antenna, the spacing is chosen to be 22.9 mm, which is $0.45\lambda$. This is slightly larger than the $0.3\lambda$ to $0.4\lambda$ range specified for Yagi-Uda design in Ref. [23]. To achieve an omnidirectional pattern in the $H$-plane, a symmetric layout is employed. Unlike a traditional Yagi-Uda antenna, the reflector is removed, but the reflective and directive nature of the parasitic elements still remains. The radiation patterns in the $H$-plane with different numbers of elements

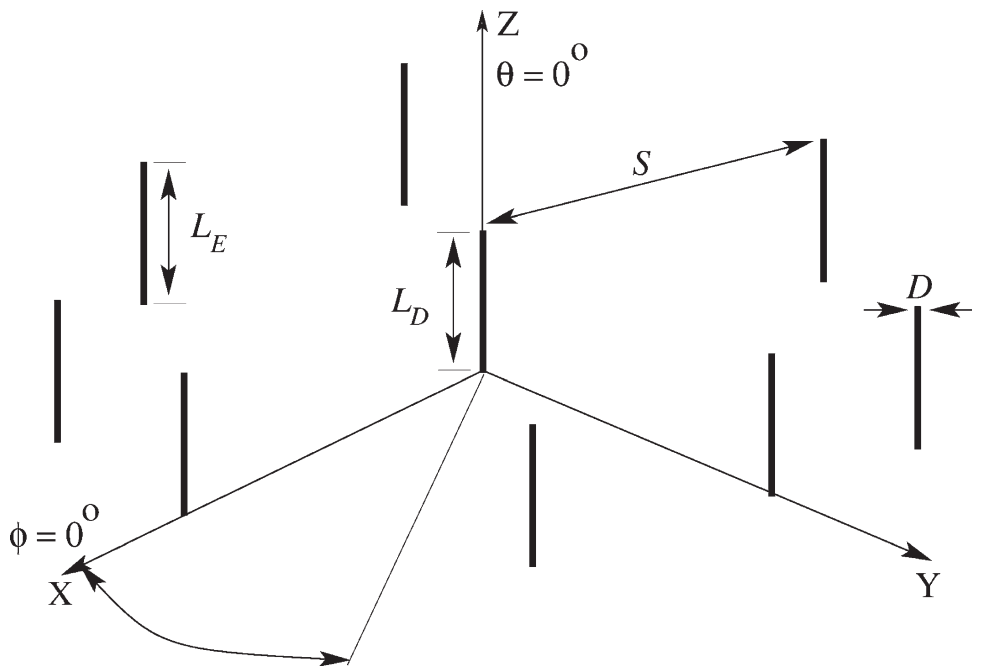


**Figure 1** An ideal setup of the proposed monopole antenna with eight parasitic elements.

are given in Figure 4. From Figure 4, it is observed that the parasitic elements are considerably directive while maintaining a high level of gain. However, the apparent nulls with a 2 dB difference from the peak level that occur for antennas with few parasitic elements are not acceptable for vehicle-to-vehicle communications. Increasing the number of elements and arranging them symmetrically is necessary to obtain the desired omnidirectional pattern with some sacrifice of the peak gain.

### III. FEED NETWORK BOARD DESIGN

As a part of the antenna system, the feed network board will have the following functions. First, it must match the impedance of the antenna to the characteristic impedance of a standard 50-Ω cable (i.e., it mitigates reflections due to the impedance mismatch between the driven monopole element and the 50-Ω transmission line). Second, it provides mechanical support for the antenna elements. Finally, it is the electrical and mechanical connection between the antenna and the body of the vehicle.

Figure 5 illustrates the bottom side of the board structure, and board details are listed in Table III. The height and width of the board are determined based on the dimensions of the antenna. Board material properties are chosen based on commercial availability, and these are also represented in Table III. The screws shown in Figure 5 are necessary to fix the board to the system's metal base and to mitigate any spurious modes that may exist due to parallel plate modes.

As stated previously, Figure 5 shows the bottom side of the feed network board, where there is a grounded coplanar waveguide (GCPW) trace that connects the antenna radiator element to an SMA connector. The antenna will be installed on the top side of the board. The driven element will be setup through the board in the center and connected to the end of the impedance transformer.

The transformer used for this design is a quarter-wave transformer [24] to match between the antenna input impedance and the 50-Ω transmission line. The two

**TABLE II Design Parameters of the Antenna**

| Symbol | Value (mm) |
|---|---|
| $L_D$ | 10.6 |
| $L_E$ | 10.2 |
| $S$ | 22.9 |
| $D$ | 0.4 |

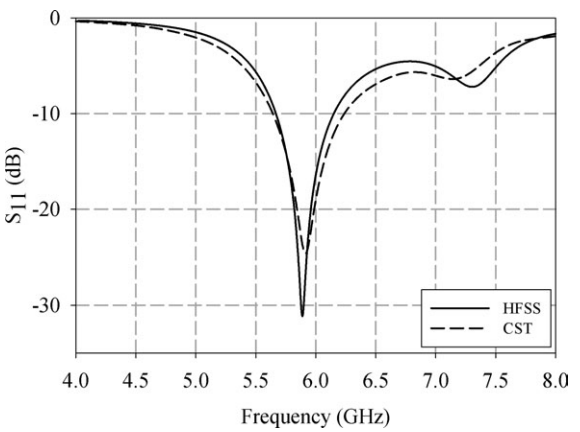


**Figure 2** Return loss of the proposed antenna with the ideal setup.

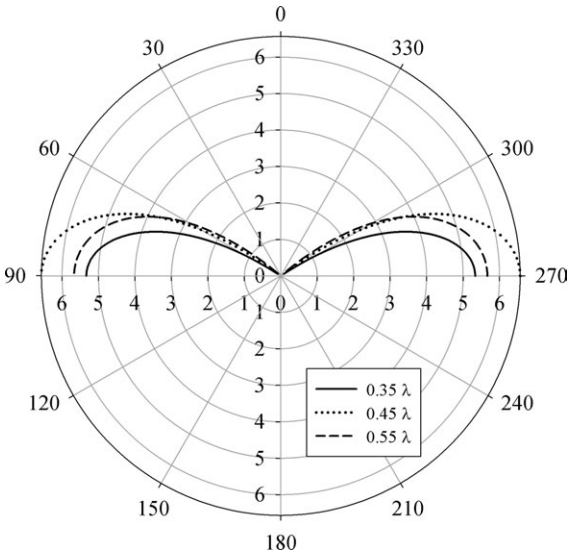


**Figure 3** *E*-plane gain patterns in dB at 5.9 GHz with varying spacing (*S*).

parameters that need to be calculated to realize this design are the necessary characteristic impedance of the transformer and the length of the trace.

The characteristic impedance of the transformer is given by [24]:

$$Z_1 = \sqrt{Z_o R_L} \tag{1}$$

where $Z_1$ is the characteristic impedance of the quarter-wave transformer, $Z_o$ is the characteristic impedance of the transmission line (i.e., 50 Ω), and $R_L$ is the resistance of the driven element (36.8 Ω). This results in a 43-Ω characteristic impedance for the quarter-wave transformer.

The length of the transformer is quarter wavelength at 5.9 GHz. This is expressed as follows:

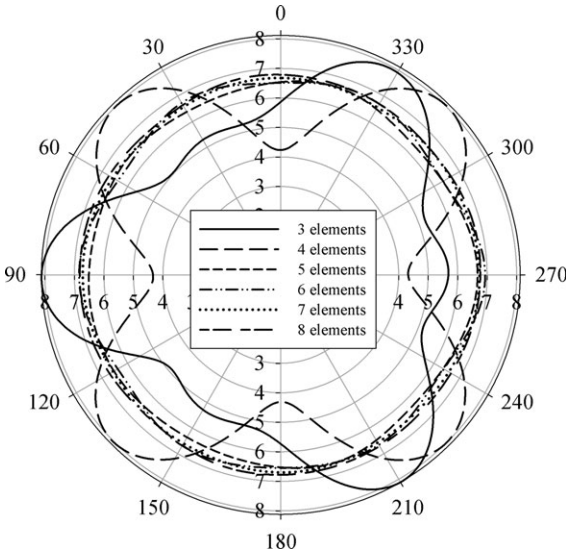


**Figure 4** *H*-plane gain patterns in dB at 5.9 GHz with different number of parasitic elements.

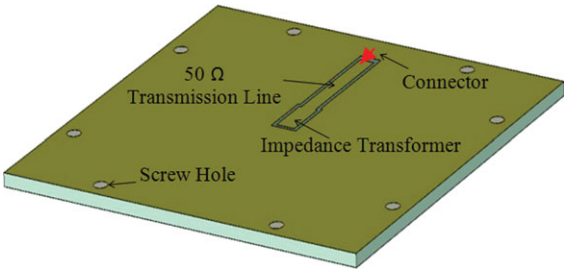


**Figure 5** Feed network configuration. [Color figure can be viewed in the online issue, which is available at wileyonlinelibrary.com.]

$$\frac{\lambda}{4} = \frac{c}{4f_o\sqrt{\varepsilon_{\text{eff}}}} \tag{2}$$

where $c$ is the speed of light in free space, $f_o$ is the center frequency of the antenna, and $\varepsilon_{\text{eff}}$ is the effective dielectric constant for GCPW. The effective dielectric constant can be calculated from equations in Ref. [25] based on the dielectric constant of the substrate, the dimensions of the trace, and the air gaps beside the trace.

For this design, the effective dielectric constant of 4.04 was calculated, and substituted into Eq. (2) results in a transformer length of 6.3 mm. To achieve the desired 50-Ω impedance of the main trace and the 43-Ω impedance of the quarter-wave transformer, the trace width and the air gap width were adjusted leading to the optimum values listed in Table III. The scattering parameters for the quarter-wave impedance transformer between the antenna input impedance and the 50-Ω line are shown in Figure 6. It is clearly seen that the transformer provides a good matching at 5.9 GHz.

## IV. ANTENNA INTEGRATION

Figure 7 depicts the proposed fully integrated antenna, consisting of the ideal antenna integrated with the feed network board and the metal base. The metal base, which will be placed on the car roof, acts as a mechanical support and electrically conducting part by attaching to the feed network board through the use of eight screws shown in Figure 5.

Using CST Microwave Studio, Figure 8 compares the reflection coefficient ($S_{11}$) response of the ideal antenna of

**TABLE III Feed Network Board Details**

| Parameter | Value |
|---|---|
| Board dimension | 55 mm × 55 mm |
| Substrate dielectric constant | 6.15 |
| Substrate thickness | 1.524 mm |
| Copper thickness | 0.035 mm |
| 50 Ω T-line trace width | 1.8 mm |
| 50 Ω T-line gap width | 0.8 mm |
| 50 Ω T-line length | 15 mm |
| Impedance transformer trace width | 2.2 mm |
| Impedance transformer gap width | 0.6 mm |
| Impedance transformer length | 6.3 mm |

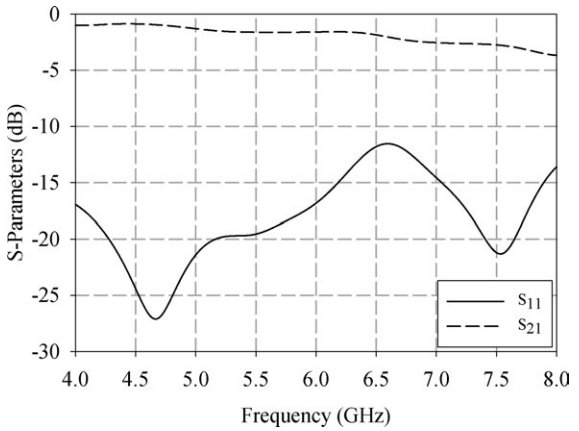


**Figure 6** S-parameters results of the quarter-wave transformer.

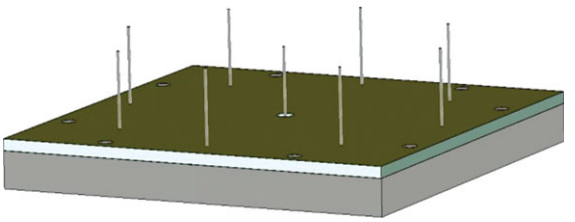

**Figure 7** Proposed fully integrated antenna (i.e., combination of the ideal antenna, the feed network board, and a metal base). [Color figure can be viewed in the online issue, which is available at wileyonlinelibrary.com.]

Figure 1 to that of the proposed fully integrated antenna of Figure 7. It is observed that the metal base of the antenna slightly affects the bandwidth, which still fully covers the target band 5.85–5.925 GHz.

Figures 9(a) and 9(b) compare the radiation patterns for the proposed fully integrated antenna with the antenna in its ideal setup at 5.9 GHz in *H*- and *E*-planes, respectively. The *H*-plane pattern illustrates that an almost omnidirectional radiation pattern is achieved in a manner similar to the conventional dipole antennas. Compared with the radiation pattern of the ideal antenna in the *H*-plane, the metal base changes the pattern slightly but does not reduce the gain in any direction. On the other hand, the *E*-plane of the proposed antenna introduces tiny side lobes less than 1 dB. The *E*-plane and *H*-plane radiation patterns demonstrate a peak gain of 6.5 and 7.5 dB for the ideal antenna and the proposed fully integrated antenna, respectively.

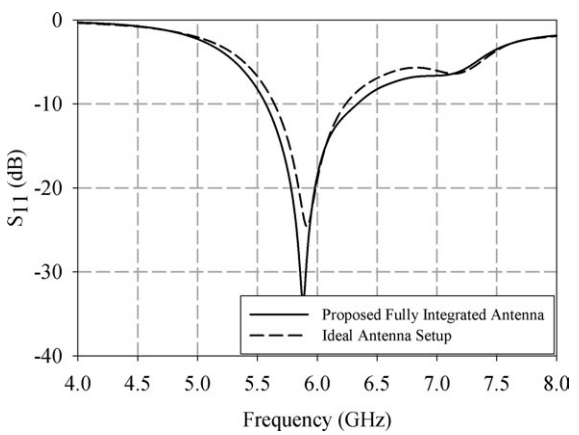


**Figure 8** Return loss of both ideal and fully integrated antenna.

## V. CONCLUSIONS

In this article, a low-profile, low-cost wire antenna with improved gain is introduced. A specific feed network with a metallic base is designed for this antenna. The proposed

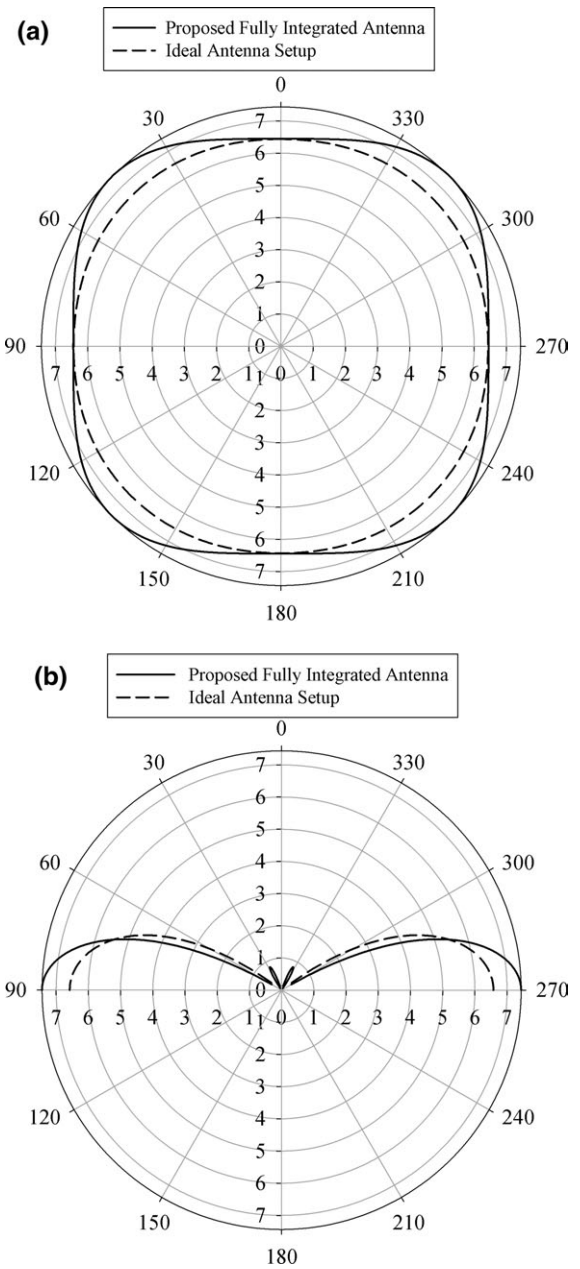


**Figure 9** Evaluated antenna gain pattern in dB for both ideal and fully integrated antennas at 5.9 GHz: (a) *H*-plane and (b) *E*-plane.

antenna comprises of a monopole wire antenna surrounded by eight parasitic elements to generate the antenna omnidirectional radiation pattern. The antenna array is also integrated with the feed network board and a supportive metal box. The performance of the proposed integrated antenna is evaluated, and the results indicate that the reflection coefficient ($S_{11}$) level is sufficient over the entire DSRC frequency band. Moreover, the proposed antenna exhibits an omnidirectional *H*-plane pattern, which is essential for vehicle-to-vehicle and vehicle-to-infrastructure DSRC communications.

## ACKNOWLEDGMENTS

The authors gratefully acknowledge the support from National Science Foundation (NSF) in the form of the NSF Engineering Design and Innovation (EDI) grant 1000744. The authors thank Dr. Mansoor Alam, Professor and Chair of the EECS Department, and Dr. Christina Bloebaum, NSF EDI Program Director.

## REFERENCES

1. M. Chiaberge, New trends and developments in automotive system engineering, InTech, Rijeka, Croatia, 2011.
2. IEEE Standard for Information Technology, local and metropolitan area networks-Specific requirements, Part 11: Wireless LAN Medium Access Control (MAC) and Physical Layer (PHY) Specifications Amendment 6: Wireless Access in Vehicular Environments, 2010. Available at: http://standards.ieee.org/findstds/standard/802.11p-2010.html.
3. G. Karagiannis, O. Altintas, E. Ekici, G. Heijenk, B. Jarupan, K. Lin, and T. Weil, Vehicular networking: A survey and tutorial on requirements, architectures, challenges, standards and solutions, IEEE Commun Surveys Tuts 13 (2011), 584–616.
4. H. Brueckmann, Theory and performance of vehicular center-fed whip antenna, IRE Trans Veh Commun 9 (1960), 10–20.
5. H. Brueckmann, Improved wide-band VHF whip antenna, IEEE Trans Veh Commun 15 (1966), 15–32.
6. Z. Novacek, Radiation of a whip antenna on the car body, Radioelectronika, 17th International Conference, Brno, June 2007, pp. 1–4.
7. H. Lindenmeier, J. Hopf, and L. Reiter, Active AM-FM windshield antenna with equivalent performance to the whip now as standard equipment in car production, IEEE International Symposium on Antennas and Propagation Society, Munich, Germany, June 1985, pp. 621–624.
8. L. Low, R. Langley, R. Breden, and P. Callaghan, Hidden automotive antenna performance and simulation, IEEE Trans Antennas Propag 54 (2006), 3707–3712.
9. J. Schaffner, H. Hsu, H. Song, and T. Talty, Pattern study of tilted dash mounted PCS band and AMPS band antennas, IEEE International Symposium on Antennas and Propagation Society, Malibu, CA, July 2005, pp. 463–466.
10. Mariottini, M. Albani, E. Toniolo, D. Amatori, and S. Maci, Design of a compact GPS and SDARS integrated antenna for automotive applications, IEEE Antennas Wirel Propag Lett 9 (2010), 405–408.
11. R. Leelaratne and R. Langley, Multiband PIFA vehicle telematics antennas, IEEE Trans Veh Technol 54 (2005), 477–485.
12. H. Jairam, Novel blade antenna using microstrip patch elements, in 19th European Microwave Conference, London, UK, 1989, pp. 1118–1122.
13. A. Walbeoff and R. Langley, Multiband PCB antenna, Proceedings of IEE Microwaves, Antennas and Propagation, Centre, Sittingbourne, UK, Dec. 2005, pp. 471–475.
14. A. Secord and W. Tilston, A new colinear antenna array, IRE Trans Veh Commun 9 (1960), 36–46.
15. J.-F. Kiang, Analysis of linear coaxial antennas, IEEE Trans Antennas Propag 46 (1998), 636–642.
16. K. Luk and S. Wong, A printed high-gain monopole antenna for indoor wireless LANs, Microwave Opt Technol Lett 41 (2004), 177–180.
17. S. Uda and Y. Mushiake, Yagi-Uda antenna, Research Institute of Electrical Communication, Tohoku University, Japan, 1954.
18. J. Brianeze, A. Sodre', and H. Herna'ndez-Figueroa, Tridimensional yagi antenna: Shaping radiation pattern with a non-planar array, IET Microwaves Antennas Propag 4 (2010), 1434–1441.
19. D. Nascimento, R. Schildberg, and J. da, S. Lacava, Low-cost Yagi-Uda monopole array, IEEE International Symposium on Antennas and Propagation Society, San Diega, CA, July 2008, pp. 1–4.
20. R. Schlub and D. Thiel, Switched parasitic antenna on a finite ground plane with conductive sleeve, IEEE Trans Antennas Propag 52 (2004), 1343–1347.
21. M. Weiner, S. Cruze, C.-C. Li, and W. Wilson, Monopole elements on circular ground planes, Artech House, Massachusetts, 1987.
22. Y. Kim, C. Song, I. Koo, H. Choi, and S. Lee, Design of a double-looped monopole array antenna for a DSRC system raodside base station, Microwave Opt Technol Lett 37 (2003), 74–77.
23. C. Balanis, Antenna theory: Analysis and design, 3rd ed., Wiley, Hoboken, New Jersey, 2005.
24. D. Pozar, Microwave engineering, 3rd ed., Wiley, NewYork, 2005.
25. B. Wadell, Transmission line design handbook, Artech House, Massachusetts, 1991.

## BIOGRAPHIES

**Michael Westrick** received his Bachelor of Science in Electrical Engineering from the University of Toledo in 2010. From 2010 to 2011, he was a Graduate Research Assistant at the University of Toledo. Currently, he is working toward his Master of Science in Electrical Engineering at the University of Toledo. His research interests include high frequency antenna design and modeling in vehicular environments and super wide band (SWB) antenna design.

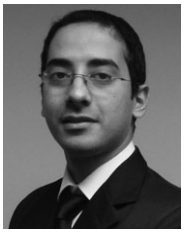

**Mohammad Almalkawi** received his B.Sc. in Telecommunications Engineering (with honors) from Yarmouk University, Jordan, in 2007, his M.Sc. in Electrical Engineering from South Dakota School of Mines & Technology, SD, USA in 2009, and his Ph.D. in Engineering from the University of Toledo, OH, USA in 2011. In the summer of 2011, he was an Intern with Freescale Semiconductor, Inc. working on modeling RF/Microwave components for

the development of product-level models. He is a Postdoctoral Research Associate in the EECS Department at the University of Toledo. His current research interests include RF/Microwave circuit design and modeling, UWB antennas, and electromagnetic compatibility.

**Vijay Devabhaktuni** received his B.Eng. in EEE and his M.Sc. in Physics from BITS, Pilani, in 1996, and his Ph.D. in Electronics from Carleton University, Canada, in 2003. He was awarded the Carleton University's senate medal at the PhD level. During 2003–2004, he held the NSERC (Natural Sciences and Engg. Research Council) postdoctoral fellowship and spent the tenure researching at the University of Calgary. In spring of 2005, he taught at Penn State Erie Behrend. During 2005–2008, he held the prestigious Canada Research Chair in Computer-Aided High-Frequency Modeling and Design at Concordia University, Montreal. Since 2008, he is an Associate Professor in the EECS Department at the University of Toledo. His R&D interests include applied electromagnetics, biomedical applications of wireless sensor networks, computer aided design, device modeling, image processing, infrastructure monitoring, neural networks, optimization methods, RF/microwave devices, and virtual reality applications. In these areas, he secured external funding close to $4M (sponsoring agencies include AFOSR, CFI, ODOT, NASA, NSERC, NSF, as well as industry). He co-authored 100 peer-reviewed papers, and is advising 17 MS/PhD students and 3 PDFs. He has won several teaching excellence awards in Canada and USA. He currently serves as the Associate Editor of the International Journal of RF and Microwave Computer-Aided Engineering. He is a registered member of the Association of Professional Engineers, Geologists and Geophysicists of Alberta and is a Senior Member of the IEEE.

**Chuck Bunting** (S-1989, M-1994, SM-2011) was born in Virginia Beach, Virginia. In 1994, he received his M.S. in Electrical Engineering from Virginia Polytechnic Institute and State University (Virginia Tech) From 1994 to 2001, he was an Assistant/Associate Professor at Old Dominion University in the Department of Engineering Technology where he worked closely with NASA Langley Research Center on electromagnetic field penetration in aircraft structures and reverberation chamber simulation using finite element techniques. In the Fall of 2001 he joined the faculty of Oklahoma State University as an Associate Professor and was promoted to full professor in August of 2011. His research focus on modeling and validation has led to numerous research grants and contracts with both industry and government. His engineering education research has led to national visibility in impacting large courses with problem-based learning. His significant professional activities in the IEEE Electromagnetic Compatibility Society include membership on the board of directors, designation as a distinguished lecturer, and offices on numerous standards and technical committees.